

Higgs-photon associated production at hadron colliders

Ali Abbasabadi¹, David Bowser-Chao², Duane A. Dicus³ and Wayne W. Repko⁴

¹*Department of Physical Sciences, Ferris State University, Big Rapids, Michigan 49307*

²*Department of Physics, University of Illinois at Chicago, Chicago, Illinois 60607*

³*Center for Particle Physics and Department of Physics University of Texas, Austin, Texas 78712*

⁴*Department of Physics and Astronomy Michigan State University, East Lansing, Michigan 48824*

(July 3, 2021)

Abstract

We present cross sections for the reactions $p\bar{p} \rightarrow H\gamma$ and $pp \rightarrow H\gamma$ arising from the subprocess $q\bar{q} \rightarrow H\gamma$. The calculation includes the complete one-loop contribution from all light quarks as well as the tree contributions from the light quarks and c and b quarks. These are the main sources of Higgs-photon associated production at hadron colliders. At Tevatron energies, the cross section is typically between 0.1fb and 1.0 fb for $80 \text{ GeV} \leq m_H \leq 160 \text{ GeV}$, while at LHC energies it exceeds about 2.0 fb over the same range of m_H . While substantial, these cross sections are not large enough to produce a signal which is discernable above the backgrounds from $q\bar{q} \rightarrow b\bar{b}\gamma$ and $gg \rightarrow b\bar{b}\gamma$.

14.80.Bn, 13.85.-t, 12.15.Ji

I. INTRODUCTION

The production of intermediate mass Higgs bosons at hadron colliders arises primarily from the gluon fusion process $gg \rightarrow H$, which is dominated by the top quark loop [1]. Depending on the collider energy, there can also be a substantial contribution from the gauge boson fusion processes $W^+W^-, ZZ \rightarrow H$ [2]. For Higgs boson masses m_H less than $2m_W$, detection of the Higgs via its dominant decay mode $H \rightarrow b\bar{b}$ must contend with a large background from $gg \rightarrow b\bar{b}$. The production of Higgs bosons in association with a gauge boson, specifically Z, W^\pm [3,4] or a photon [5,6], is potentially helpful in dealing with these backgrounds, although at a significant cost in the rate.

In this report, we examine the possibility of using Higgs-photon associated production in hadron collisions as a means of studying properties of the Higgs boson. The main source of the $H\gamma$ final state is quark-antiquark annihilation. Two-gluon annihilation, which accounts for single H production, is forbidden by Furry's theorem because the gluons are in a color singlet state. For light quarks, the direct annihilation into $H\gamma$ is suppressed by the ratio m_q/m_W and is negligible. This means that one-loop electroweak corrections involving W 's, Z 's and top quarks dominate the light quark contribution to $q\bar{q} \rightarrow H\gamma$. The diagrams involved in the one-loop quark-antiquark annihilation calculation are similar to those encountered in the calculation of $e\bar{e} \rightarrow H\gamma$, which has been performed for the Standard Model [5,6] and its supersymmetric generalization [7]. As in the case of $\mu\bar{\mu} \rightarrow H\gamma$ [8,9], there are also tree-level contributions from $c\bar{c}$ and $b\bar{b}$ annihilation, which are enhanced by their larger couplings but suppressed by parton distribution function effects.

In the next section, we outline the extension of our previous tree [9] and one-loop results [6] to $q\bar{q} \rightarrow H\gamma$. This is followed by a discussion.

II. OUTLINE OF THE CALCULATION

A. Tree-level amplitudes

The tree-level diagrams are illustrated in Fig. 1 and the resulting amplitude is

$$\mathcal{M}^{\text{tree}} = \frac{e_q g m_q}{2m_W} \left[-i \left(\frac{p_1 \cdot \epsilon^*}{p_1 \cdot k} - \frac{p_2 \cdot \epsilon^*}{p_2 \cdot k} \right) \bar{v}(p_2) u(p_1) + \left(\frac{1}{2p_1 \cdot k} + \frac{1}{2p_2 \cdot k} \right) \bar{v}(p_2) \sigma_{\mu\nu} k_\nu u(p_1) \epsilon_\mu^* \right], \quad (1)$$

where p_1 is the momentum of the quark, p_2 the momentum of the antiquark, k the momentum of the γ and ϵ its polarization and e_q is the quark charge in units of the proton charge. For massless quarks, only the helicity non-flip contributions from the factors $\bar{v}(p_2)u(p_1)$ and $\bar{v}(p_2)\sigma_{\mu\nu}u(p_1)$ are non-zero. Thus, we expect the helicity flip tree amplitudes to contain a factor of order m_q/E relative to the non-flip amplitudes. Explicitly, we find,

$$\mathcal{M}_{\lambda_1 \lambda_2 \lambda_\gamma}^{\text{tree}} = -i \frac{e_q g m_q}{\sqrt{2} m_W} \left(\frac{1}{2p_1 \cdot k} + \frac{1}{2p_2 \cdot k} \right) \begin{cases} \sin \theta [\lambda_\gamma (2|\mathbf{p}|^2 - E\omega) + |\mathbf{p}|\omega] & , \lambda_1 \lambda_2 = ++ \\ \sin \theta [\lambda_\gamma (2|\mathbf{p}|^2 - E\omega) - |\mathbf{p}|\omega] & , \lambda_1 \lambda_2 = -- \\ m_q \omega (1 + \lambda_\gamma \cos \theta) & , \lambda_1 \lambda_2 = +- \\ m_q \omega (1 - \lambda_\gamma \cos \theta) & , \lambda_1 \lambda_2 = -+ \end{cases}, \quad (2)$$

where E is the quark energy in the center of mass, $|\mathbf{p}| = \sqrt{E^2 - m_q^2}$, ω is the photon energy, θ is the photon scattering angle and $\lambda_\gamma = \pm 1$ is the photon helicity. It can be seen that the helicity flip amplitudes have an additional factor of m_q .

B. One-loop amplitudes

The one-loop amplitudes for $q\bar{q} \rightarrow H\gamma$ receive contributions from pole diagrams involving virtual photon and Z exchange and from various box diagrams containing quarks, gauge bosons and/or Goldstone bosons. There are also double pole diagrams whose contribution vanishes. This is illustrated in Fig. 1. The main difference between $e\bar{e}$ annihilation and $q\bar{q}$ annihilation occurs in the crossed box diagram in the last row of Fig. 1. Since both members of a quark doublet are charged, there are additional crossed box diagrams containing W 's. This contribution can be obtained from our Z box results by merely changing the coupling and replacing m_Z by m_W .

In the non-linear gauges we chose [6], the full amplitude consists of four separately gauge invariant terms: a photon pole, a Z pole, Z boxes and W boxes. These amplitudes can be written as

$$\mathcal{M}_{\text{pole}}^\gamma = \frac{\alpha^2 m_W}{\sin\theta_W} \bar{v}(p_2)\gamma_\mu u(p_1) \left(\frac{\delta_{\mu\nu} k \cdot (p_1 + p_2) - k_\mu (p_1 + p_2)_\nu}{s} \right) \hat{\epsilon}_\nu(k) \mathcal{A}_\gamma(s), \quad (3)$$

$$\mathcal{M}_{\text{pole}}^Z = \frac{\alpha^2 m_W}{\sin^3\theta_W} \bar{v}(p_2)\gamma_\mu (v_q + \gamma_5) u(p_2) \left(\frac{\delta_{\mu\nu} k \cdot (p_1 + p_2) - k_\mu (p_1 + p_2)_\nu}{(s - m_Z^2) + im_Z \Gamma_Z} \right) \hat{\epsilon}_\nu(k) \mathcal{A}_Z(s), \quad (4)$$

$$\begin{aligned} \mathcal{M}_{\text{box}}^Z = & -\frac{\alpha^2 m_Z}{4 \sin^3\theta_W \cos^3\theta_W} \bar{v}(p_2)\gamma_\mu (v_q + \gamma_5)^2 u(p_1) \{ [\delta_{\mu\nu} k \cdot p_1 - k_\mu (p_1)_\nu] \mathcal{B}_Z(s, t, u) \\ & + [\delta_{\mu\nu} k \cdot p_2 - k_\mu (p_2)_\nu] \mathcal{B}_Z(s, u, t) \} \hat{\epsilon}_\nu(k), \end{aligned} \quad (5)$$

$$\begin{aligned} \mathcal{M}_{\text{box}}^W = & \frac{\alpha^2 m_W}{2 \sin^3\theta_W} \bar{v}(p_2)\gamma_\mu (1 + \gamma_5)^2 u(p_1) \{ [\delta_{\mu\nu} k \cdot p_1 - k_\mu (p_1)_\nu] \mathcal{B}_W(s, t, u) \\ & + [\delta_{\mu\nu} k \cdot p_2 - k_\mu (p_2)_\nu] \mathcal{B}_W(s, u, t) \} \hat{\epsilon}_\nu(k), \end{aligned} \quad (6)$$

where $s = -(p_1 + p_2)^2$, $t = -(k + p_1)^2$ and $u = -(k + p_2)^2$. Here, v_q denotes the $q\bar{q}Z$ vector coupling constant, $v_q = 1 - 4|e_q| \sin^2\theta_W$. In terms of the scalar functions defined in the appendices of our previous paper [6], we have [10]

$$\begin{aligned} \mathcal{A}_\gamma(s) = & -e_q \left\{ 4 \left(6 + \frac{m_H^2}{m_W^2} \right) C_{23}(s, m_H^2, m_W^2) - 16 C_0(s, m_H^2, m_W^2) \right. \\ & \left. - \frac{16}{3} \frac{m_t^2}{m_W^2} \left(4 C_{23}(s, m_H^2, m_t^2) - C_0(s, m_H^2, m_t^2) \right) \right\}, \end{aligned} \quad (7)$$

$$\begin{aligned} \mathcal{A}_Z(s) = & -2I_3 \left\{ \left(5 - \tan^2\theta_W + \frac{m_H^2}{2m_W^2} (1 - \tan^2\theta_W) \right) C_{23}(s, m_H^2, m_W^2) \right. \\ & + (\tan^2\theta_W - 3) C_0(s, m_H^2, m_W^2) \\ & \left. - \frac{1}{2} \frac{m_t^2}{m_W^2} \frac{1 - (8/3) \sin^2\theta_W}{\cos^2\theta_W} \left(4 C_{23}(s, m_H^2, m_t^2) - C_0(s, m_H^2, m_t^2) \right) \right\}, \end{aligned} \quad (8)$$

$$\mathcal{B}_Z(s, t, u) = -\tilde{e}_q A(s, t, u), \quad (9)$$

$$\mathcal{B}_W(s, t, u) = -2I_3 [A_1(s, t, u) + A_2(s, u, t)] + \tilde{e}_q A'(s, t, u), \quad (10)$$

with I_3 denoting the third component of the *external* quark weak isospin, m_t being the top quark mass and the prime denoting the replacement $m_Z \rightarrow m_W$. \tilde{e}_q is the charge of the *internal* quark in units of the proton charge. In this case, it is the helicity flip contributions from the factors $\bar{v}(p_2)\gamma_\mu u(p_1)$ and $\bar{v}(p_2)\gamma_\mu\gamma_5 u(p_1)$ which survive in the $m_q \rightarrow 0$ limit. This can be seen by noting that, in the center of mass, we have

$$\bar{v}_+(p_2)\gamma_\nu u_+(p_1) = im_q(p_2 - p_1)_\nu/|\mathbf{p}|, \quad (11a)$$

$$\bar{v}_+(p_2)\gamma_\nu\gamma_5 u_+(p_1) = im_q(p_2 + p_1)_\nu/E, \quad (11b)$$

$$\bar{v}_+(p_2)\gamma_\nu u_-(p_1) = -2\sqrt{2}iE\xi_\nu^{(-)}, \quad (11c)$$

$$\bar{v}_+(p_2)\gamma_\nu\gamma_5 u_-(p_1) = -2\sqrt{2}i|\mathbf{p}|\xi_\nu^{(-)}, \quad (11d)$$

with $\xi_\nu^{(-)} = (1, -i, 0, 0)/\sqrt{2}$. If we define $\mathcal{M}^{\text{loop}}$ as

$$\mathcal{M}^{\text{loop}} = \mathcal{M}_{\text{pole}}^\gamma + \mathcal{M}_{\text{pole}}^Z + \mathcal{M}_{\text{box}}^Z + \mathcal{M}_{\text{box}}^W, \quad (12)$$

then $\mathcal{M}^{\text{loop}}$ is predominantly helicity flip.

C. Differential cross section

The differential cross section $d\sigma(q\bar{q} \rightarrow H\gamma)/d\Omega_\gamma$ is

$$\frac{d\sigma(q\bar{q} \rightarrow H\gamma)}{d\Omega_\gamma} = \frac{1}{256\pi^2} \frac{s - m_H^2}{s^2} \sum_{\text{helicity}} |\mathcal{M}|^2, \quad (13)$$

where the invariant amplitude $\mathcal{M} = \mathcal{M}^{\text{tree}} + \mathcal{M}^{\text{loop}}$. Because of the helicity structure discussed above, the interference terms turn out to be negligible and one can simply add the tree and one-loop cross sections.

To obtain the collider cross sections, we convolute Eq. (13) with the appropriate quark and antiquark distribution functions using

$$\frac{d\sigma}{dm_{H\gamma}^2} = \frac{1}{s} \int_\tau^1 \frac{dx}{x} f_q(x) f_{\bar{q}}(\tau/x) \int_{-z_0}^{z_1} dz \frac{d\sigma(q\bar{q} \rightarrow H\gamma)}{dz}. \quad (14)$$

Here, $\tau = m_{H\gamma}^2/s$, $z = \cos\theta_\gamma$ and z_0 and z_1 are determined by the choice of the rapidity and transverse momentum cuts. We used CTEQ3-1M parton distribution functions [11] and imposed a rapidity cut of 2.5 and a transverse momentum cut of 10 GeV on both the Higgs boson and the photon.

III. DISCUSSION

The total cross section for $p\bar{p}(pp) \rightarrow H\gamma$ is illustrated in Fig. 2 for an upgraded Tevatron energy of 2.0 TeV (left panel) and an LHC energy of 14 TeV (right panel). In each case,

we show the tree contributions from light quarks (u, d, s), light quarks plus the c quark and light quarks plus c and b quarks. In addition, the loop contribution from the light quarks is shown. The loop contributions from the c and b quarks are negligible. As asserted in the Introduction, Fig. 2 confirms that the light quark tree contribution can always be neglected. Interestingly, the largest tree contribution is due to the c quark for both the Tevatron and the LHC, and the b quark contribution is always important. At the Tevatron energy, the loop diagrams contribute about as much as the tree diagrams, while, for the LHC, the tree diagrams dominate.

In our calculation of the heavy quark tree contributions, we simply convoluted the cross section for $Q\bar{Q} \rightarrow H\gamma$ with the complete heavy parton distribution functions [11], instead of subtracting from them the lowest order logarithmic correction to avoid potential double counting of higher order gluonic contributions [12,13]. Based on an earlier study of Higgs boson production at the SSC [14], this procedure is likely to somewhat overestimate the heavy quark fusion contribution. The effects of QCD corrections have not been considered, although some of these, in particular the K factor, usually increase the heavy quark cross sections [15]. We have not included top quark fusion in our results since the top quark is almost certainly too massive to be treated as a parton at LHC energies.

Although there are non-negligible numbers of events for a Tevatron with an upgraded luminosity of 20 - 30fb⁻¹/year [16] or the LHC with a design luminosity of 100fb⁻¹/year, the background to the signal $p\bar{p}(pp) \rightarrow H\gamma \rightarrow b\bar{b}\gamma$ must be considered. To do this, we have calculated the direct production of the $b\bar{b}\gamma$ final state arising from the channels $p\bar{p}(pp) \rightarrow q\bar{q} \rightarrow b\bar{b}\gamma$ [17] and $p\bar{p}(pp) \rightarrow gg \rightarrow b\bar{b}\gamma$. In Table I, the background contributions are shown for cuts on the $b\bar{b}$ invariant mass $m_{b\bar{b}}$ in the vicinity of $m_H = 100$ GeV and 200 GeV and rapidity cuts $y_{\max} = 1.0$ and 2.5 on the b, \bar{b} and γ . In addition to these cuts, we require the separation ΔR between the γ and the b and the γ and the \bar{b} to be greater than 0.4, the transverse momenta of the b, \bar{b} and γ to be greater than 15 GeV, and the $b\bar{b}\gamma$ invariant mass to be greater than 170 GeV. The latter two cuts reduce the background in the $m_H = 100$ GeV region by about a factor of 5. They reduce the loop signal by about 40% at $\sqrt{s} = 1.8$ TeV and 14 TeV, but the corresponding reduction in the tree contribution is a factor of 15 at 1.8 TeV and a factor of 6.8 at 14 TeV. Thus the tree contribution, though substantial, is difficult to isolate.

The background is compared to the signal in Table II for Higgs boson masses of 100 GeV and 200 GeV. Despite the application of numerous cuts, it appears that the background is prohibitively large for the observation of a Higgs boson with Standard Model couplings produced in association with a photon.

Finally, to determine the sensitivity of associated production to changes in the $t\bar{t}H$ coupling, we computed the cross section including a factor λ multiplying the Standard Model coupling [18]. For a 2 TeV Tevatron upgrade, this effect is illustrated in Fig. 3 as a function of λ . The most obvious effect is the uniform decrease in the cross section as λ varies from $\lambda = 0$ to the Standard Model value at $\lambda = 1.0$. With increasing λ , the cross sections eventually exceed the Standard Model result. The enhancement in the cross section for larger values of λ is still not sufficient to produce favorable S/\sqrt{B} value. For example, for $\lambda = 10$ and $m_H = 100$ GeV, the cuts used for Table II give $S/\sqrt{B} \sim .22$. It is clear that any anomalous $H\gamma$ coupling must result in a cross section of several femtobarns and a fairly isotropic angular distribution in order to produce a signal that will survive the cuts

required to reduce the $b\bar{b}\gamma$ background.

ACKNOWLEDGMENTS

We would like to thank G. Kane for several helpful conversations and Wu-Ki Tung for informative discussions about heavy quark parton distribution functions. This research was supported in part by the U.S. Department of Energy under Contract No. DE-FG013-93ER40757 and in part by the National Science Foundation under Grant No. PHY-93-07980.

REFERENCES

- [1] J. F. Gunion, H. E. Haber, G. Kane, and S. Dawson, *The Higgs Hunter's Guide* (Addison-Wesley, Menlo Park, CA, 1990).
- [2] S. Petcov and D. R. T. Jones, Phys. Lett. **B84**, 440 (1979); R. N. Cahn and S. Dawson, Phys. Lett. **B136**, 196 (1984), **B138**, 464 (1984) (E); G. L. Kane, W. W. Repko and W. B. Rolnick, Phys. Lett. **B148**, 367 (1984); S. Dawson, Nucl. Phys. **B249**, 42 (1985).
- [3] J. D. Bjorken, *in* Proceeding of the SLAC Summer Institute on Particle Physics, Stanford, CA (1976); SLAC Pub **1866** (1977).
- [4] S. Mrenna and G. L. Kane, *Possible detection of a Higgs boson at higher luminosity hadron colliders*, hep-ph/9406337 (1994) (unpublished).
- [5] A. Barroso, J. Pulido and J. C. Romão, Nucl. Phys. **B267**, 509 (1986).
- [6] A. Abbasabadi, D. Bowser-Chao, D. A. Dicus and W. W. Repko, Phys. Rev. D **52**, 3919 (1995).
- [7] A. Djouadi, V. Driesen, W. Hollick and J. Rosiek, University of Karlsruhe preprint KA-TP-21-96, hep-ph/9609420.
- [8] V. A. Litvin and F. F. Tikhonin, *Associated production of $H\gamma$ and HZ pairs at $\mu^+\mu^-$ collisions*, hep-ph/9704417 (1997).
- [9] A. Abbasabadi, D. Bowser-Chao, D. A. Dicus and W. W. Repko, Phys. Rev. D **57**, 550 (1998).
- [10] Equations (7) and (8) contain an additional factor of 2 in the top quark contribution compared to Ref. [6].
- [11] CTEQ Collaboration: H. L. Lai, *et al.*, Phys. Rev. D **51**, 4763 (1995).
- [12] R. M. Barnett, H. E. Haber and D. E. Soper, Nucl. Phys. **B306**, 697 (1988).
- [13] F. I. Olness and W.-K. Tung, Nucl. Phys. **B308**, 813 (1988).
- [14] D. A. Dicus S. Willenbrock, Phys. Rev. D **39**, 751 (1989).
- [15] J. Dai, J. F. Gunion and R. Vega, Phys. Lett. B **345**, 29 (1995).
- [16] P. P. Bagley, *et al.*, *Summary of the TEV33 Working Group*, FERMILAB-CONF 96-392, Oct. 1996.
- [17] The $q\bar{q} \rightarrow b\bar{b}\gamma$ amplitudes were adapted from the amplitudes for $e\bar{e} \rightarrow \mu\bar{\mu}\gamma$, see: F. Berends *et al.*, Nucl. Phys. **B206**, 61 (1982); Z. Xu, D-H Zhang, and L. Chang, Nucl. Phys. **B291**, 392 (1987).
- [18] H. E. Haber, G. L. Kane and T. Sterling, Nucl. Phys. **B161**, 493 (1979).

TABLES

\sqrt{s}	y_{\max}	$98.5 < m_{b\bar{b}} < 101.5$	$99 < m_{b\bar{b}} < 101$	$198.5 < m_{b\bar{b}} < 201.5$
1.8 TeV	2.5	41.9 fb	28.7 fb	20.0 fb
1.8 TeV	1.0	5.57 fb	3.73 fb	4.35 fb
14 TeV	2.5	340 fb	227 fb	276 fb
14 TeV	1.0	29.7 fb	19.8 fb	25.4 fb

TABLE I. Cross sections for the backgrounds $p\bar{p}(pp) \rightarrow q\bar{q} \rightarrow \gamma b\bar{b}$ and $p\bar{p}(pp) \rightarrow gg \rightarrow \gamma b\bar{b}$ are given for several cuts on the $b\bar{b}$ invariant mass $m_{b\bar{b}}$ (in GeV), a cut y_{\max} on the rapidities of the γ , the b and the \bar{b} , and other cuts discussed in the text.

\sqrt{s}	y_{\max}	$\sigma(m_H = 100 \text{ GeV})$	S/\sqrt{B}	$\sigma(m_H = 200 \text{ GeV})$	S/\sqrt{B}
1.8 TeV	2.5	4.41×10^{-2} fb	.05	9.01×10^{-3} fb	.01
1.8 TeV	1.0	1.79×10^{-2} fb	.05	4.57×10^{-3} fb	.02
14 TeV	2.5	1.22 fb	.66	9.13×10^{-1} fb	.55
14 TeV	1.0	2.43×10^{-1} fb	.46	2.96×10^{-1} fb	.59

TABLE II. The cross sections for the associated production of 100 GeV and 200 GeV Higgs bosons are shown together with the ratio of the signal to the square root of the background (S/\sqrt{B}) for the Tevatron and the LHC. A luminosity of 50 fb^{-1} is assumed at $\sqrt{s} = 1.8 \text{ TeV}$ and 100 fb^{-1} at $\sqrt{s} = 14 \text{ TeV}$. The cuts used are discussed in the text.

FIGURES

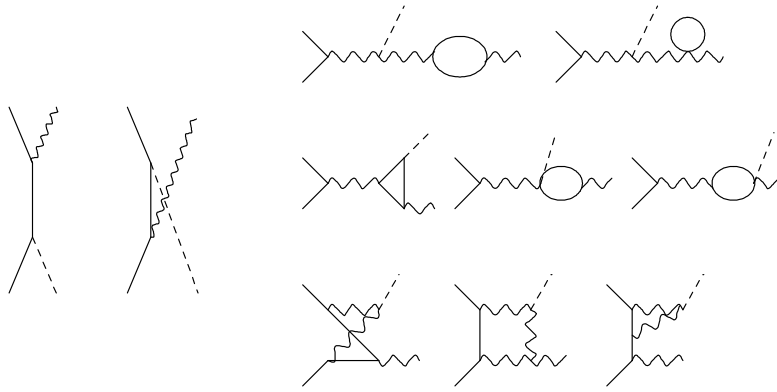


FIG. 1. Typical diagrams for the tree and one-loop contributions are shown. An external solid line represents a quark, a wavy line a gauge boson, a dashed line a Higgs boson and an internal solid line a quark, gauge boson, Goldstone boson or ghost.

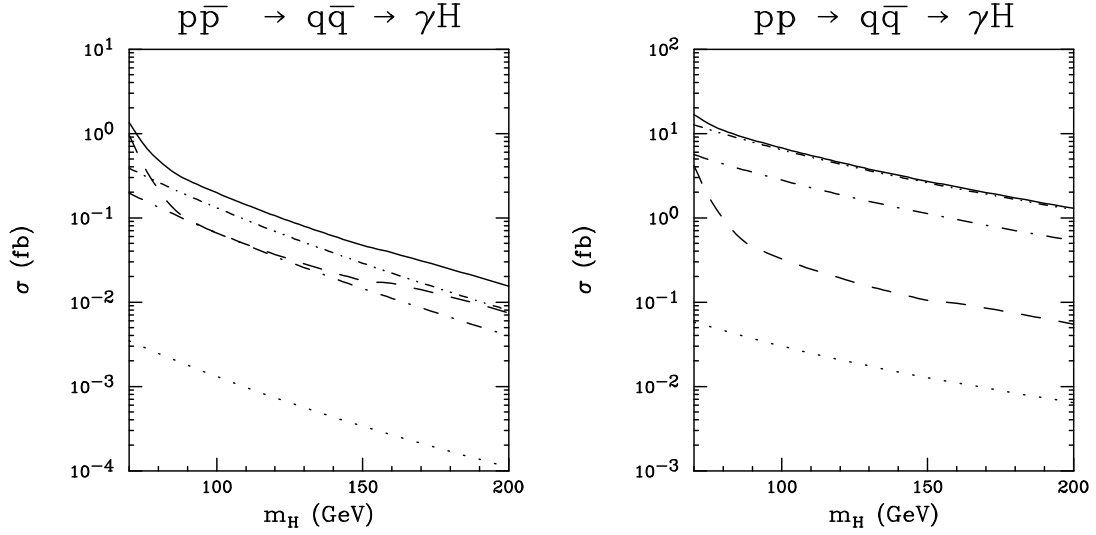


FIG. 2. The total cross section for $H\gamma$ production from $q\bar{q}$ annihilation in $p\bar{p}$ and pp scattering is shown for a Tevatron energy of 2 TeV and an LHC energy of 14 TeV. In each panel, the dotted line is the light quark tree contribution, the dot-dashed line is the light quark plus c quark tree contribution, the dot-dot-dashed line is the light quark plus c and b tree contribution and the dashed line is the loop contribution. The solid line is the sum of the tree and loop contributions. The cuts used are discussed in the text.

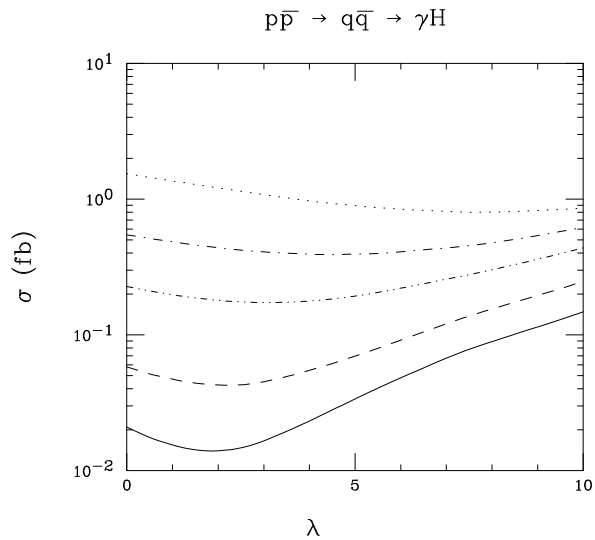


FIG. 3. The total cross section (tree + loop) for $H\gamma$ production from $q\bar{q}$ annihilation in $p\bar{p}$ scattering is shown as a function of the $t\bar{t}H$ coupling (in multiples λ of the Standard Model coupling) at an upgraded Tevatron for several values of m_H . The dotted line is $m_H = 70$ GeV, the dot-dashed line $m_H = 80$ GeV, the dot-dot-dashed line $m_H = 100$ GeV, the dashed line $m_H = 150$ GeV, and the solid line $m_H = 200$ GeV.